

Metastability of hadronic compact stars

Ignazio Bombaci,¹ Prafulla K. Panda,^{2,3} Constança Providência,³ and Isaac Vidña⁴

¹*Dipartimento di Fisica “Enrico Fermi,” Università di Pisa, and INFN, Sezione di Pisa, Largo Bruno Pontecorvo 3, I-56127 Pisa, Italy*

²*Indian Association for the Cultivation of Sciences, Jadavpur, Kolkata-700 032, India*

³*Centro de Física Teórica, Department of Physics, University of Coimbra, 3004-516 Coimbra, Portugal*

⁴*Departament d'Estructura i Constituents de la Matèria. Universitat de Barcelona, Avda. Diagonal 647, E-08028 Barcelona, Spain*

(Received 13 December 2007; published 7 April 2008)

Pure hadronic compact stars, above a threshold value of their gravitational mass (central pressure), are metastable to the conversion to quark stars (hybrid or strange stars). In this paper, we present a systematic study of the metastability of pure hadronic compact stars using different relativistic models for the equation of state. In particular, we compare results for the quark-meson coupling model with those for the Glendenning-Moszkowski parametrization of the nonlinear Walecka model. For the quark-meson coupling model, we find large values ($M_{\text{cr}} = 1.6\text{--}1.9M_{\odot}$) for the critical mass of the hadronic star sequence and we find that the formation of a quark star is only possible with a soft quark matter equation of state. For the Glendenning-Moszkowski parametrization of the nonlinear Walecka model, we explore the effect of different hyperon couplings on the critical mass and on the stellar conversion energy. We find that increasing the value of the hyperon coupling constants shifts the bulk transition point for quark deconfinement to higher densities, increases the stellar metastability threshold mass and the value of the critical mass, and thus makes the formation of quark stars less likely. For the largest values of the hyperon couplings we find a critical mass which may be as high as $1.9\text{--}2.1M_{\odot}$. These stellar configurations, which contain a large central hyperon fraction ($f_{Y,\text{cr}} \sim 30\%$), would be able to describe highly massive compact stars, such as the one associated with the millisecond pulsar PSR B1516 + 02B with a mass $M = 1.94^{+0.17}_{-0.19}M_{\odot}$.

DOI: [10.1103/PhysRevD.77.083002](https://doi.org/10.1103/PhysRevD.77.083002)

PACS numbers: 97.60.Jd, 26.60.Kp, 26.60.Dd

I. INTRODUCTION

The nucleation of quark matter in neutron stars has been studied by many authors, due to its potential connection with explosive astrophysical events such as supernovae and gamma ray burst. Some of the earlier studies on quark matter nucleation (see e.g., [1–3] and references therein) dealt with thermal nucleation in hot and dense hadronic matter. In these studies, it was found that the prompt formation of a critical-size drop of quark matter via thermal activation is possible above a temperature of about 2–3 MeV. As a consequence, it was inferred that pure hadronic stars (HS) are converted to quark stars (QS) [hybrid stars (HYS) or strange stars (SS)] within the first seconds after their birth. However, neutrino trapping in the proto-neutron star phase strongly precludes the formation of a quark phase [4–7]. Then, it is possible that the compact star survives the early stages of its evolution as a pure hadronic star. In this case, the nucleation of quark matter would be triggered by quantum fluctuations in degenerate ($T = 0$) neutrino-free hadronic matter [8–15].

Quantum fluctuations could form, in principle, a drop of β -stable quark matter (hereafter the Q^{β} phase). However, this process is strongly suppressed with respect to the formation of a non- β -stable drop by a factor $\sim G_{\text{Fermi}}^{2N/3}$, where $N \sim 100\text{--}1000$ is the number of quarks in a critical-size quark drop. This is so because the formation of a β -stable drop would involve the almost simultaneous conversion of $\sim N/3$ up (u) and down (d) quarks into strange (s) quarks. Alternatively, quantum fluctuations

can form a non- β -stable drop (hereafter the Q^* phase), in which the flavor content of the quark phase is equal to that of the β -stable hadronic phase at the same pressure [9,10,12]. Since no flavor conversion is involved, there are no suppressing Fermi factors and a Q^* drop can be nucleated much more easily. Once a critical-size Q^* drop is formed, the weak interactions will have enough time to act, changing the quark flavor fraction of the deconfined droplet to lower its energy, and a drop of the Q^{β} phase is formed. This first seed of quark matter will trigger the conversion [16–18] of the pure hadronic star to a hybrid star or to a strange star (depending on the details of the equation of state for quark matter used to model the phase transition). The stellar conversion process liberates a total energy of the order of 10^{53} erg [18].

When finite-size effects at the interface between the quark and hadron phases are taken into account, it is necessary to have an overpressure $\Delta P = P - P_0 > 0$ with respect to the bulk transition point P_0 , to create a drop of deconfined quark matter. As a consequence, pure hadronic stars with values of the central pressure larger than P_0 are metastable to the decay (conversion) to hybrid stars or to strange stars [11–15]. The mean lifetime of the metastable stellar configuration is related to the time needed to nucleate the first drop of quark matter in the stellar center and depends dramatically on the value of the stellar central pressure [11–15].

The possibility of having in nature both metastable hadronic stars and stable quark stars has led the authors of Ref. [12] to extend the concept of limiting mass of a

“neutron star” with respect to the *classical* one introduced by Oppenheimer and Volkoff [19]. Since metastable HS with a “short” *mean lifetime* are very unlikely to be observed, the extended concept of limiting mass has been introduced in view of the comparison with the values of the mass of compact stars deduced from direct astrophysical observation (see Sec. 3.1 of Ref. [12] for the definition of the *limiting mass* M_{lim} of compact stars in the case of metastable pure hadronic stars).

As it is well known, neutron star mass measurements give one of the most stringent tests on the overall *stiffness* of dense matter equation of state (EOS). Recent measurements of post-Keplerian orbital parameters in relativistic binary stellar systems (containing millisecond pulsars) give strong evidence for the existence of highly massive “neutron stars.” For example, the compact star associated with the millisecond pulsar PSR B1516 + 02B in the globular cluster NGC 5904 (M5) has a mass $M = 1.94^{+0.17}_{-0.19} M_{\odot}$ (1σ) [20]. In the case of PSR J1748-2021B, a millisecond pulsar in the globular cluster NGC 6440, the measured mass is $M = 2.74^{+0.41}_{-0.51} M_{\odot}$ (2σ) [21]. These measurements challenge most of the existing models for dense matter EOS.

In this work, we carry out a systematic study of the properties of metastable hadronic compact stars obtained within different relativistic mean-field models for the equation of state of hadronic matter. In particular, we compare the predictions of the quark-meson coupling (QMC) model [22,23] with those of the nonlinear Walecka model (NLWM) [24] parametrizations given by Glendenning-Moszkowski (GM) [25].

For the quark phase we have adopted a phenomenological EOS [26] which is based on the MIT bag model for hadrons. The parameters here are the mass m_s of the strange quark, the so-called pressure of the vacuum B (bag constant) and the quantum chromodynamics structure constant α_s . For all the quark matter models used in the present work, we take $m_u = m_d = 0$, $m_s = 150$ MeV, and $\alpha_s = 0$.

In the QMC model quark degrees of freedom are explicitly taken into account: baryons are described as a system of nonoverlapping MIT bags which interact through the effective scalar and vector mean fields. The coupling constants are defined at the quark level. An attractive aspect of the model is that different phases of hadronic matter, from very low to very high baryon densities, can be described within the same underlying model, namely, the MIT bag model: matter at low densities is a system of nucleons interacting through meson fields, with quarks and gluons confined within MIT bag; at very high density one expects that baryons and mesons dissolve and the entire system of quarks and gluons becomes confined within a single, big MIT bag.

In the case of the Glendenning-Moszkowski EOS [25], we have paid special attention to the role played by the

hyperon-meson couplings. In fact, all previous works on metastable hadronic stars [11–15] have uniquely considered the case of “low” values for these quantities ($x_{\sigma} = 0.6$ for the ratio between the hyperon- σ -meson to nucleon- σ -meson coupling). As it is well known, larger values of the hyperon-meson couplings (constrained by the empirical binding energy of the Λ particle in nuclear matter) make the EOS stiffer and increase the value of the Oppenheimer-Volkoff mass for the hadronic stellar sequence [25]. In addition, as we demonstrate in the present work, increasing the values of the hyperon-meson couplings shifts the bulk transition point for quark deconfinement to higher densities and increments the value of the *critical mass* M_{cr} (see Refs. [11–13] and Sec. III for the explicit definition of this quantity) for the hadronic stellar sequence. Thus our study is relevant in connection with the recent measurements of highly massive “neutron stars” mentioned above.

A brief review of the nonlinear Walecka and QMC models is given in Sec. II. The quantum nucleation of a quark matter drop inside hadronic matter is briefly reviewed in Sec. III. Our main results are presented in Sec. IV, whereas the main conclusions are given in Sec. V.

II. FORMALISM

In the present section we review the models used in this work, namely, the GM parametrizations [25] of the NLWM and the quark-meson coupling (QMC) model including hyperons.

A. Nonlinear Walecka model

The Lagrangian density, including the baryonic octet, in terms of the scalar σ , the vector-isoscalar ω_{μ} , and the vector-isovector $\vec{\rho}_{\mu}$ meson fields, reads (see e.g. [4,27,28])

$$\mathcal{L} = \mathcal{L}_{\text{hadrons}} + \mathcal{L}_{\text{leptons}}, \quad (1)$$

where the hadronic contribution is

$$\mathcal{L}_{\text{hadrons}} = \mathcal{L}_{\text{baryons}} + \mathcal{L}_{\text{mesons}} \quad (2)$$

with

$$\mathcal{L}_{\text{baryons}} = \sum_{\text{baryons}} \bar{\psi} [\gamma^{\mu} D_{\mu} - M_B^*] \psi, \quad (3)$$

where

$$D_{\mu} = i\partial_{\mu} - g_{\omega B} \omega_{\mu} - g_{\rho B} \vec{t}_B \cdot \vec{\rho}_{\mu} \quad (4)$$

and $M_B^* = M_B - g_{\sigma B} \sigma$. The quantity \vec{t}_B designates the isospin of baryon B . The mesonic contribution reads

$$\mathcal{L}_{\text{mesons}} = \mathcal{L}_{\sigma} + \mathcal{L}_{\omega} + \mathcal{L}_{\rho} \quad (5)$$

with

$$\mathcal{L}_{\sigma} = \frac{1}{2} (\partial_{\mu} \sigma \partial^{\mu} \sigma - m_{\sigma}^2 \sigma^2) + \frac{1}{3!} \kappa \sigma^3 + \frac{1}{4!} \lambda \sigma^4, \quad (6)$$

$$\mathcal{L}_\omega = -\frac{1}{4}\Omega_{\mu\nu}\Omega^{\mu\nu} + \frac{1}{2}m_\omega^2\omega_\mu\omega^\mu, \quad (7)$$

$$\Omega_{\mu\nu} = \partial_\mu\omega_\nu - \partial_\nu\omega_\mu,$$

$$\mathcal{L}_\rho = -\frac{1}{4}\vec{B}_{\mu\nu} \cdot \vec{B}^{\mu\nu} + \frac{1}{2}m_\rho^2\vec{\rho}_\mu \cdot \vec{\rho}^\mu, \quad (8)$$

$$\vec{B}_{\mu\nu} = \partial_\mu\vec{\rho}_\nu - \partial_\nu\vec{\rho}_\mu - g_\rho(\vec{\rho}_\mu \times \vec{\rho}_\nu).$$

For the lepton contribution we take

$$\mathcal{L}_{\text{leptons}} = \sum_{\text{leptons}} \bar{\psi}_l(i\gamma_\mu\partial^\mu - m_l)\psi_l, \quad (9)$$

where the sum is over electrons and muons. In uniform matter, we get for the baryon Fermi energy $\epsilon_{FB} = g_{\omega B}\omega_0 + g_{\rho B}t_{3B}\rho_{03} + \sqrt{k_{FB}^2 + M_B^{*2}}$, with the baryon effective mass $M_B^* = M - g_{\sigma B}\sigma$.

We will use the GM1 and GM3 parametrizations of NLWM [25] both fitted to the bulk properties of nuclear matter: for GM1 (GM3) the compressibility is 300 (240) MeV and the effective mass at saturation $M^* = 0.7M$ ($M^* = 0.78M$). The inclusion of hyperons involves new couplings, the hyperon-nucleon couplings: $g_{\sigma B} = x_{\sigma B}g_\sigma$, $g_{\omega B} = x_{\omega B}g_\omega$, $g_{\rho B} = x_{\rho B}g_\rho$. For nucleons we take $x_{\sigma B}, x_{\omega B}, x_{\rho B} = 1$ and for hyperons we will consider the couplings proposed by Glendenning and Moszkowski [25]. They have considered the binding energy of the Λ in nuclear matter B_Λ

$$\left(\frac{B_\Lambda}{A}\right) = -28 \text{ MeV} = x_\omega g_\omega \omega_0 - x_\sigma g_\sigma \sigma \quad (10)$$

to establish a relation between x_σ and x_ω . Moreover, known neutron star masses restrict x_σ to the range 0.6–0.8. We will take $x_\rho = x_\sigma$ and will consider $x_\sigma = 0.6, 0.7, 0.8$.

B. Quark-meson coupling model for hadronic matter

In the QMC model, the nucleon in nuclear medium is assumed to be a static spherical MIT bag in which quarks interact with the scalar and vector fields σ , ω , and ρ and these fields are treated as classical fields in the mean-field approximation [22,23]. The quark field $\psi_q(x)$ inside the bag then satisfies the equation of motion:

$$\left[i\not{D} - (m_q^0 - g_\sigma^q\sigma) - g_\omega^q\omega\gamma^0 + \frac{1}{2}g_\rho^q\tau_z\rho_{03} \right] \times \psi_q(x) = 0, \quad q = u, d, s, \quad (11)$$

where m_q^0 is the current quark mass and g_σ^q , g_ω^q , and g_ρ^q denote the quark-meson coupling constants. The normalized ground state for a quark in the bag is given by

$$\psi_q(\mathbf{r}, t) = \mathcal{N}_q \exp(-i\epsilon_q t/R_B) \begin{pmatrix} j_0(x_q r/R_B) \\ i\beta_q \vec{\sigma} \cdot \hat{r} j_1(x_q r/R_B) \end{pmatrix} \times \frac{\chi_q}{\sqrt{4\pi}}, \quad (12)$$

where

$$\epsilon_q = \Omega_q + R_B \left(g_\omega^q \omega + \frac{1}{2} g_\rho^q \tau_z \rho_{03} \right);$$

$$\beta_q = \sqrt{\frac{\Omega_q - R_B m_q^*}{\Omega_q + R_B m_q^*}}, \quad (13)$$

with the normalization factor given by

$$\mathcal{N}_q^{-2} = 2R_B^3 j_0^2(x_q) [\Omega_q(\Omega_q - 1) + R_B m_q^*/2] / x_q^2, \quad (14)$$

where $\Omega_q \equiv \sqrt{x_q^2 + (R_B m_q^*)^2}$, $m_q^* = m_q^0 - g_\sigma^q\sigma$, R_B is the bag radius of the baryon, and χ_q is the quark spinor. The quantities ψ_q , ϵ_q , β_q , \mathcal{N}_q , Ω_q , m_q^* all depend on the baryon considered. The bag eigenvalue x_q is determined by the boundary condition at the bag surface,

$$j_0(x_q) = \beta_q j_1(x_q). \quad (15)$$

The energy of a static bag describing baryon B consisting of three ground state quarks can be expressed as

$$E_B^{\text{bag}} = \sum_q n_q \frac{\Omega_q}{R_B} - \frac{Z_B}{R_B} + \frac{4}{3} \pi R_B^3 B_B, \quad (16)$$

where Z_B is a parameter which accounts for zero-point motion and B_B is the bag constant. The effective mass of a nucleon bag at rest is taken to be $M_B^* = E_B^{\text{bag}}$. The equilibrium condition for the bag is obtained by minimizing the effective mass M_B^* with respect to the bag radius

$$\frac{dM_B^*}{dR_B^*} = 0. \quad (17)$$

For the QMC model, the equations of motion for the meson fields in uniform static matter are given by

$$m_\sigma^2 \sigma = \sum_B g_{\sigma B} C_B(\sigma) \frac{2J_B + 1}{2\pi^2} \times \int_0^{k_B} \frac{M_B^*(\sigma)}{[k^2 + M_B^{*2}(\sigma)]^{1/2}} k^2 dk, \quad (18)$$

$$m_\omega^2 \omega_0 = \sum_B g_{\omega B} (2J_B + 1) k_B^3 / (6\pi^2), \quad (19)$$

$$m_\rho^2 \rho_{03} = \sum_B g_{\rho B} I_{3B} (2J_B + 1) k_B^3 / (6\pi^2). \quad (20)$$

In the above equations J_B , I_{3B} , and k_B are, respectively, the spin, isospin projection, and the Fermi momentum of the baryon species B . For the hyperon couplings we take $x_\omega = 0.78$ and $x_\rho = 0.7$. The coupling x_σ is an output of the

model and is approximately equal to 0.7. Note that the s quark is unaffected by the σ and ω mesons, i.e. $g_\sigma^s = g_\omega^s = 0$.

In Eq. (18) we have

$$g_{\sigma B} C_B(\sigma) = -\frac{\partial M_B^*(\sigma)}{\partial \sigma} = -\frac{\partial E_B^{\text{bag}}}{\partial \sigma} = \sum_{q=u,d} n_q g_\sigma^q S_B(\sigma), \quad (21)$$

where

$$S_B(\sigma) = \int_{\text{bag}} d\mathbf{r} \bar{\psi}_q \psi_q = \frac{\Omega_q/2 + R_B m_q^*(\Omega_q - 1)}{\Omega_q(\Omega_q - 1) + R_B m_q^*/2};$$

$$q \equiv (u, d). \quad (22)$$

The total energy density and the pressure including the leptons can be obtained from the grand canonical potential and they read

$$\begin{aligned} \varepsilon = & \frac{1}{2} m_\sigma^2 \sigma^2 + \frac{1}{2} m_\omega^2 \omega_0^2 + \frac{1}{2} m_\rho^2 \rho_{03}^2 \\ & + \sum_B \frac{2J_B + 1}{2\pi^2} \int_0^{k_B} k^2 dk [k^2 + M_B^{*2}(\sigma)]^{1/2} \\ & + \sum_l \frac{1}{\pi^2} \int_0^{k_l} k^2 dk [k^2 + m_l^2]^{1/2}, \end{aligned} \quad (23)$$

$$\begin{aligned} P = & -\frac{1}{2} m_\sigma^2 \sigma^2 + \frac{1}{2} m_\omega^2 \omega_0^2 + \frac{1}{2} m_\rho^2 \rho_{03}^2 \\ & + \frac{1}{3} \sum_B \frac{2J_B + 1}{2\pi^2} \int_0^{k_B} \frac{k^4 dk}{[k^2 + M_B^{*2}(\sigma)]^{1/2}} \\ & + \frac{1}{3} \sum_l \frac{1}{\pi^2} \int_0^{k_l} \frac{k^4 dk}{[k^2 + m_l^2]^{1/2}}. \end{aligned} \quad (24)$$

For the bag radius we take $R_N = 0.6$ fm. The two unknowns Z_N and B_N for nucleons are obtained by fitting the nucleon mass $M = 939$ MeV and enforcing the stability condition for the bag at free space. The values obtained are $Z_N = 3.98699$ and $B_N^{1/4} = 211.303$ MeV for $m_u = m_d = 0$ MeV, and $Z_N = 4.00506$ and $B_N^{1/4} = 210.854$ MeV for $m_u = m_d = 5.5$ MeV. We take these bag values B_B for all baryons and the parameters Z_B and R_B of the other baryons are obtained by reproducing their physical masses in free space and again enforcing the stability condition for their bags. Note that for a fixed bag value, the equilibrium condition in free space results in an increase of the bag radius and a decrease of the parameters Z_B for the heavier baryons. The set of parameters used in the present work is given in Ref. [29].

Next we fit the quark-meson coupling constants g_σ^q , $g_\omega = 3g_\omega^q$, and $g_\rho = g_\rho^q$ for the nucleon to obtain the correct saturation properties of the nuclear matter, $E_B \equiv \epsilon/\rho - M = -15.7$ MeV at $\rho = \rho_0 = 0.15 \text{ fm}^{-3}$, $a_{\text{sym}} = 32.5$ MeV, $K = 257$ MeV, and $M^* = 0.774M$. We have $g_\sigma^q = 5.957$, $g_{\omega N} = 8.981$, and $g_{\rho N} = 8.651$. We take the

standard values for the meson masses, $m_\sigma = 550$ MeV, $m_\omega = 783$ MeV, and $m_\rho = 770$ MeV.

III. QUANTUM NUCLEATION OF QUARK MATTER IN HADRON STARS

Let us consider a pure hadronic star whose central pressure (density) is increasing due to spin-down or due to mass accretion (from a companion or from the interstellar medium). As the central pressure approaches the deconfinement threshold pressure P_0 (see Fig. 2), a drop of non- β -stable quark matter (Q^*), but with flavor content equal to that of the β -stable hadronic phase, can be formed in the central region of the star. The process of drop formation is regulated by its quantum fluctuations in the potential well created from the difference in the Gibbs free energies of the hadron and quark phases [9–11],

$$U(\mathcal{R}) = \frac{4}{3} \pi n_{b,Q^*} (\mu_{Q^*} - \mu_H) \mathcal{R}^3 + 4\pi \sigma \mathcal{R}^2, \quad (25)$$

where \mathcal{R} is the radius of the Q^* droplet (supposed to be spherical), n_{b,Q^*} is the quark baryon number density, μ_{Q^*} and μ_H are the quark and hadron chemical potentials at a fixed pressure P , and σ is the surface tension for the surface separating the hadron from the Q^* phase. Notice that μ is the same as the bulk Gibbs energy per baryon $g = (P + \epsilon)/n_B = (\sum_i \mu_i n_i)/n_B$. Notice also that we have neglected the term associated with the curvature energy, and also the terms connected with the electrostatic energy, since they are known to introduce small corrections [10,12]. The value of the surface tension σ for the interface separating the quark and hadron phase is poorly known and typically values used in the literature range within $10\text{--}50 \text{ MeV fm}^{-2}$ [10,30].

The time needed to form the first drop (nucleation time) can be straightforwardly evaluated within a semiclassical approach [9,10]. First one computes, in the Wentzel-Kramers-Brillouin approximation, the ground state energy E_0 , and the oscillation frequency ν_0 of the drop in the potential well $U(\mathcal{R})$. Then, the probability of tunneling is given by

$$p_0 = \exp\left[-\frac{A(E_0)}{\hbar}\right], \quad (26)$$

where A is the action under the potential barrier which in a relativistic framework reads

$$A(E) = \frac{2}{c} \int_{\mathcal{R}_-}^{\mathcal{R}_+} \sqrt{[2\mathcal{M}(\mathcal{R})c^2 + E - U(\mathcal{R})][U(\mathcal{R}) - E]}, \quad (27)$$

with \mathcal{R}_\pm being the classical turning points and

$$\mathcal{M}(\mathcal{R}) = 4\pi \rho_H \left(1 - \frac{n_{b,Q^*}}{n_H}\right)^2 \mathcal{R}^3 \quad (28)$$

being the droplet effective mass, with ρ_H and n_H the

hadron energy density and the hadron baryon number density, respectively. The nucleation time is then equal to

$$\tau = (\nu_0 p_0 N_c)^{-1}, \quad (29)$$

where N_c is the number of virtual centers of droplet formation in the star. A simple estimation gives $N_c \sim 10^{48}$ [9,10]. The uncertainty in the value of N_c is expected to be within 1 or 2 orders of magnitude. In any case, all the qualitative features of our scenario will not be affected by this uncertainty. As a consequence of the surface effects it is necessary to have an overpressure $\Delta P = P - P_0 > 0$ with respect to the bulk transition point P_0 to create a drop of deconfinement quark matter in the hadronic environment. The higher the overpressure, the easier to nucleate the first drop of Q^* matter. In other words, the higher the mass of the metastable pure hadronic star, the shorter the time to nucleate a quark matter drop at the center of the star.

In order to explore the astrophysical implications of quark matter nucleation, following Refs. [11,12], we introduce the concept of *critical mass* for the hadronic star sequence. The critical mass M_{cr} is the value of the gravitational mass of a metastable hadronic star for which the nucleation time is equal to 1 yr: $M_{\text{cr}} = M_{\text{HS}}(\tau = 1 \text{ yr})$. Therefore, pure hadronic stars with $M_{\text{HS}} > M_{\text{cr}}$ are very unlikely to be observed, while pure hadronic stars with $M_{\text{HS}} < M_{\text{cr}}$ are safe with respect to a sudden transition to quark matter. Then M_{cr} plays the role of an *effective maximum mass for the hadronic branch of compact stars* (see discussion in Ref. [12]). While the Oppenheimer-Volkov maximum mass is determined by the overall stiffness of the equation of state for hadronic matter, the value of M_{cr} will depend in addition on the properties of the intermediate non- β -stable Q^* phase.

IV. RESULTS AND DISCUSSION

In this section we present and discuss our results for stellar configurations obtained using the equation of state (EOS) models described in Sec. II. In particular, we determine the region of the pure hadronic star sequence where these compact stars are metastable, the value of the corresponding critical mass M_{cr} , and the final fate of this configuration after quark matter nucleation, i.e. whether it will evolve to a quark star or to a black hole.

In Fig. 1 the EOS for the models discussed are plotted for the range of densities of relevance for the discussion that follows. For GM1 and GM3 we have considered three different hyperon-meson couplings as discussed above. The QMC EOS corresponds approximately to $x_\sigma = 0.7$. A higher value of the hyperon couplings x_i corresponds to stiffer EOSs: at high densities we have vector dominance defined by the magnitude of x_ω, x_ρ . It is clear from Fig. 1 that the onset of hyperons (represented by the change of slope in the EOS curves) occurs for the smaller x_σ values at lower densities. The nucleonic EOS for QMC is very soft

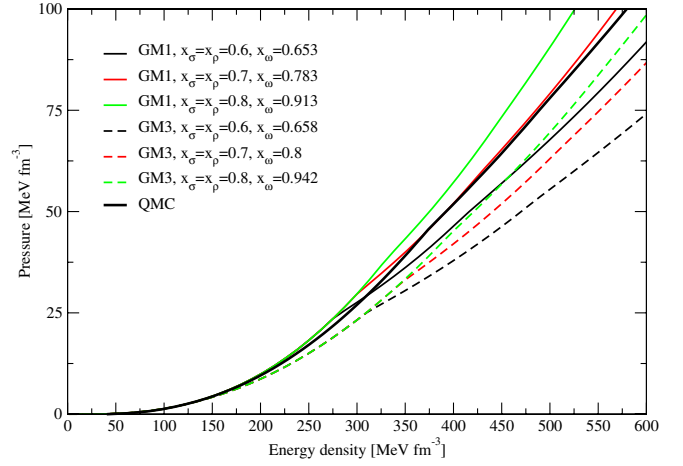


FIG. 1 (color online). Hadronic EOS for QMC and for GM1 and GM3 with the different hyperon-meson couplings discussed in the text.

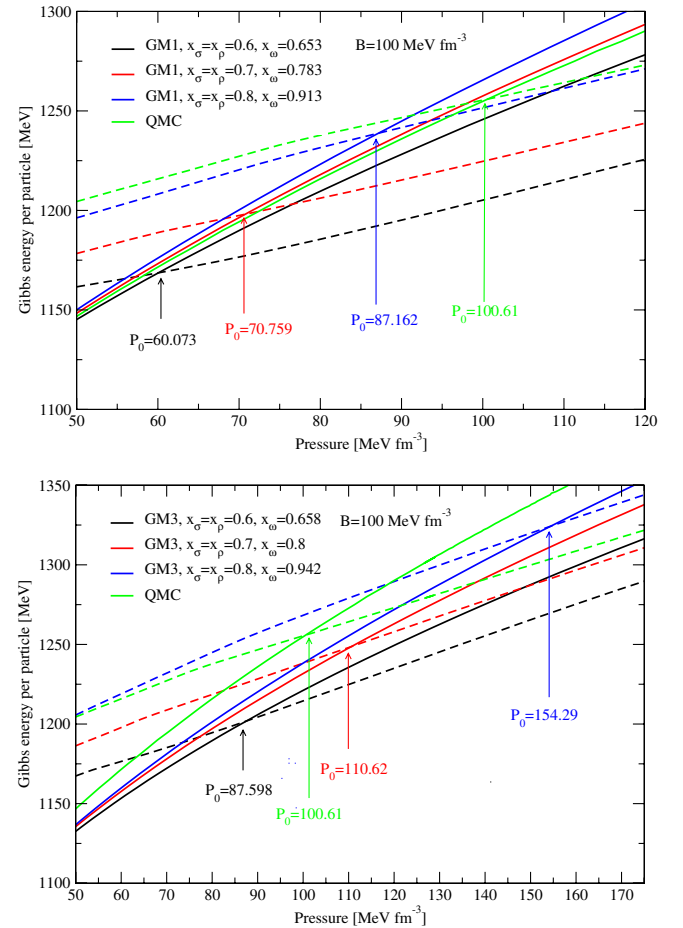


FIG. 2 (color online). The Gibbs energy per particle for the β -stable hadronic phase (continuous curves) and for the respective Q^* phase (dashed curves). The upper panel refers to the GM1 and the lower panel to the GM3 EOS. The results for the QMC model are plotted in both panels.

TABLE I. Critical masses and energy released in the conversion process of an HS into a QS, for several values of the hyperon coupling x_σ , of the bag constant B and the surface tension σ . The GM1 parameter set has been used for the hadronic EOS. The column labeled $M_{\text{QS,max}}$ ($M_{\text{QS,max}}^b$) denotes the maximum gravitational (baryonic) mass of the final QS sequence. The value of the critical gravitational (baryonic) mass of the initial HS is reported on the column labeled M_{cr} (M_{cr}^b) whereas those of the mass of the final QS and the energy released in the stellar conversion process are shown on columns labeled M_{fin} and E_{conv} respectively. BH denotes those cases in which due to the conversion the initial HS collapses into a black hole. $f_{Y,\text{cr}} = n_Y/n_B$ denotes central hyperon fraction of the critical mass star (i.e. the ratio between the total hyperon number density and the total baryon number density at the center of the critical mass star). Units of B and σ are MeV/fm³ and MeV/fm² respectively. All masses are given in solar mass units and the energy released is given in units of 10⁵¹ erg. m_s and α_s are always taken equal to 150 MeV and 0, respectively. The Oppenheimer-Volkoff maximum masses for pure hadronic stars in the case of the GM1 EOS are $M_{\text{HS,max}} = 1.790M_\odot$ (when $x_\sigma = 0.6$), $1.996M_\odot$ ($x_\sigma = 0.7$), and $2.169M_\odot$ ($x_\sigma = 0.8$).

x_σ	B	$M_{\text{QS,max}}$	$M_{\text{QS,max}}^b$	M_{cr}	M_{cr}^b	$\sigma = 10$				$\sigma = 30$			
						$f_{Y,\text{cr}}$	M_{fin}	E_{conv}	M_{cr}	M_{cr}^b	$f_{Y,\text{cr}}$	M_{fin}	E_{conv}
0.6	75	1.630	1.968	1.326	1.454	0.079	1.254	128.4	1.471	1.630	0.147	1.387	149.4
	85	1.542	1.812	1.447	1.596	0.134	1.385	110.4	1.540	1.711	0.201	1.479	125.5
	100	1.457	1.661	1.598	1.789	0.261	BH	BH	1.658	1.865	0.332	BH	BH
	150	1.447	1.601	1.770	2.010	0.527	BH	BH	1.790	2.036	0.637	BH	BH
0.7	75	1.630	1.968	1.442	1.595	0.059	1.361	144.8	1.602	1.794	0.119	1.507	169.6
	85	1.542	1.812	1.584	1.764	0.111	1.509	134.2	1.685	1.892	0.170	BH	BH
	100	1.457	1.661	1.724	1.950	0.197	BH	BH	1.791	2.036	0.253	BH	BH
	150	1.518	1.686	1.905	2.188	0.370	BH	BH	1.931	2.223	0.403	BH	BH
0.8	75	1.630	1.968	1.592	1.782	0.044	1.498	167.9	1.763	2.000	0.095	BH	BH
	85	1.542	1.812	1.735	1.954	0.085	BH	BH	1.841	2.091	0.132	BH	BH
	100	1.457	1.661	1.879	2.152	0.152	BH	BH	1.946	2.243	0.194	BH	BH
	150	1.518	1.686	2.054	2.391	0.275	BH	BH	2.081	2.429	0.299	BH	BH

and therefore the onset of hyperons occurs at quite high densities, $\varepsilon = 373.87$ MeV/fm³. As a consequence although QMC is softer than GM1 EOS at lower densities, it becomes, at higher densities, stiffer than GM1 ($x_\sigma = 0.6$) and very close to GM1 ($x_\sigma = 0.7$).

In Fig. 2, we plot the Gibbs free energy per baryon for the hadronic phase and for the corresponding Q^* phase using the various EOS models (a pair of continuous and dashed curves with the same color) considered in the

present work. It is clearly seen that in the case of the GM1 or GM3 EOS models, the lower the value of the hyperon coupling x_σ , the softer the EOS (see also Fig. 1) and the lower the pressure P_0 at the crossing between the hadronic and the Q^* phase. This will give rise to lower critical masses for the smaller x_σ values (see Tables I, II, and III). The Q^* phase is very sensitive to the particle content and it is due to this fact that, although in Fig. 2 the EOS for QMC is softer than the EOS for GM1 with

TABLE II. Same as Table I but for the GM3 parameter set for the hadronic EOS. The Oppenheimer-Volkoff maximum masses for pure hadronic stars in the case of the GM3 EOS are $M_{\text{HS,max}} = 1.554M_\odot$ (when $x_\sigma = 0.6$), $1.732M_\odot$ ($x_\sigma = 0.7$), and $1.875M_\odot$ ($x_\sigma = 0.8$).

x_σ	B	$M_{\text{QS,max}}$	$M_{\text{QS,max}}^b$	M_{cr}	M_{cr}^b	$\sigma = 10$				$\sigma = 30$			
						$f_{Y,\text{cr}}$	M_{fin}	E_{conv}	M_{cr}	M_{cr}^b	$f_{Y,\text{cr}}$	M_{fin}	E_{conv}
0.6	75	1.630	1.968	1.237	1.351	0.092	1.175	111.6	1.269	1.389	0.110	1.204	115.4
	85	1.543	1.812	1.350	1.482	0.165	1.298	91.3	1.362	1.497	0.178	1.310	92.8
	100	1.465	1.673	1.461	1.626	0.307	1.431	54.9	1.469	1.636	0.316	1.438	55.8
	150	1.487	1.658	—	—	—	—	—	—	—	—	—	—
0.7	75	1.630	1.968	1.373	1.510	0.078	1.297	136.4	1.402	1.545	0.091	1.324	140.4
	85	1.543	1.812	1.511	1.680	0.157	1.447	113.2	1.541	1.717	0.182	1.475	117.6
	100	1.465	1.673	1.610	1.806	0.253	BH	BH	1.645	1.851	0.295	BH	BH
	150	1.495	1.667	1.716	1.945	0.419	BH	BH	1.723	1.956	0.444	BH	BH
0.8	75	1.630	1.968	1.574	1.759	0.076	1.482	165.2	1.611	1.806	0.092	1.516	170.7
	85	1.543	1.812	1.694	1.913	0.143	BH	BH	1.744	1.979	0.181	BH	BH
	100	1.465	1.673	1.771	2.014	0.204	BH	BH	1.802	2.057	0.234	BH	BH
	150	1.495	1.668	1.848	2.119	0.295	BH	BH	1.856	2.131	0.309	BH	BH

TABLE III. Same as Table I but for the QMC parameter set for the hadronic EOS. The Oppenheimer-Volkoff maximum mass for pure hadronic stars in the case of the QMC EOS is $M_{\text{HS,max}} = 1.927M_{\odot}$.

B	$M_{\text{QS,max}}$	$M_{\text{QS,max}}^b$	M_{cr}	M_{cr}^b	$\sigma = 10$				$\sigma = 30$			
					$f_{Y,\text{cr}}$	M_{fin}	E_{conv}	M_{cr}	M_{cr}^b	$f_{Y,\text{cr}}$	M_{fin}	E_{conv}
75	1.630	1.968	1.587	1.768	0.044	1.488	176.8	1.694	1.903	0.090	1.585	195.8
85	1.530	1.793	1.705	1.917	0.096	BH	BH	1.768	1.998	0.145	BH	BH
100	1.454	1.656	1.790	2.027	0.168	BH	BH	1.830	2.080	0.211	BH	BH
150	1.479	1.638	1.898	2.171	0.352	BH	BH	1.909	2.187	0.377	BH	BH

$x_{\sigma} = 0.8$ and 0.7 , its crossing with the Q^* phase occurs at higher pressures. A similar observation occurs in the figure with the GM3 results. This behavior will reflect itself on values of the critical masses M_{cr} .

In Fig. 3, we show the mass-radius (MR) curve for pure HS within the QMC model for the EOS of the hadronic phase, and that for hybrid stars or strange stars for different values of the bag constant B . The configuration marked with an asterisk on the hadronic MR curves represents the hadronic star for which the central pressure is equal to the threshold value P_0 and the quark matter nucleation time is $\tau = \infty$. The full circle on the hadronic star sequence represents the critical mass configuration, in the case $\sigma = 30 \text{ MeV/fm}^2$. The full circle on the HYS (SS) mass-radius curve represents the hybrid (strange) star which is formed from the conversion of the hadronic star with $M_{\text{HS}} = M_{\text{cr}}$. We assume [18] that during the stellar conversion process the total number of baryons in the star (or in other words the stellar baryonic mass) is conserved. Thus the total energy liberated in the stellar conversion is given by the difference between the gravitational mass of the initial hadronic star ($M_{\text{in}} \equiv M_{\text{cr}}$) and that of the final hybrid or strange stellar configuration with the same baryonic mass

$$(M_{\text{fin}} \equiv M_{\text{QS}}(M_{\text{cr}}^b)):$$

$$E_{\text{conv}} = (M_{\text{in}} - M_{\text{fin}})c^2. \quad (30)$$

As we can see from Fig. 3, for the case of the QMC model, the region of metastability of pure hadronic stars (the part of the MR curve between the asterisk and the full circle) is very narrow. For this hadronic EOS, the quark star sequence can be populated only in the case of “small” values of the bag constant ($B \leq 80 \text{ MeV/fm}^3$; in this case the final star is a strange star). In all the other cases the critical mass hadronic star will form a black hole.

For comparison, in Fig. 4 we plot the MR curve obtained with the GM1 parametrization for the same surface tension ($\sigma = 30 \text{ MeV/fm}^2$) and two values for bag constant ($B = 75$ and 100 MeV/fm^3). We consider the two extreme values of the hyperon couplings studied in this work. The dots and stars have the same meaning as in Fig. 3. We see that for the cases plotted the only configuration that does not end in a black hole has the smallest bag constant and hyperon coupling considered. In the present model, however, the configuration with the central pressure P_0 and the

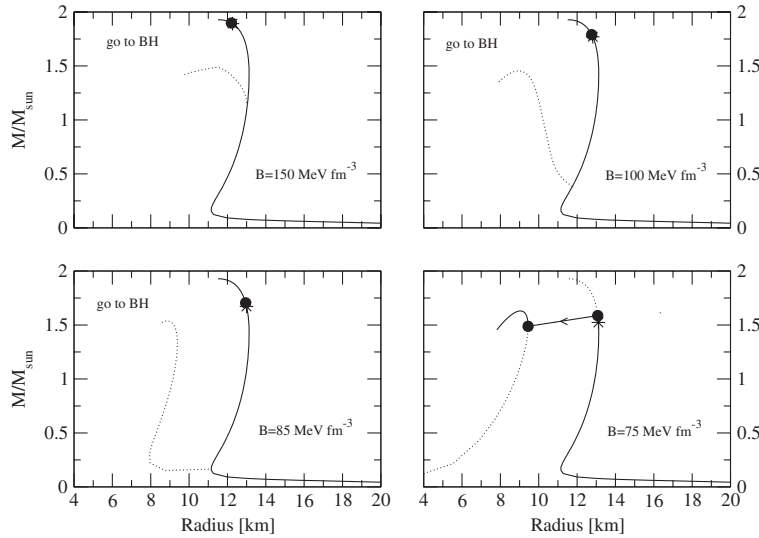


FIG. 3. Mass-radius relation for a pure HS described within the QMC model and that of the HYS or SS configurations for several values of the bag constant and $m_s = 150 \text{ MeV}$ and $\alpha_s = 0$. The configuration marked with an asterisk represents in all cases the HS for which the central pressure is equal to P_0 . The conversion process of the HS, with a gravitational mass equal to M_{cr} , into a final HYS or SS is denoted by the full circles connected by an arrow. In all the panels σ is taken equal to 30 MeV/fm^2 .

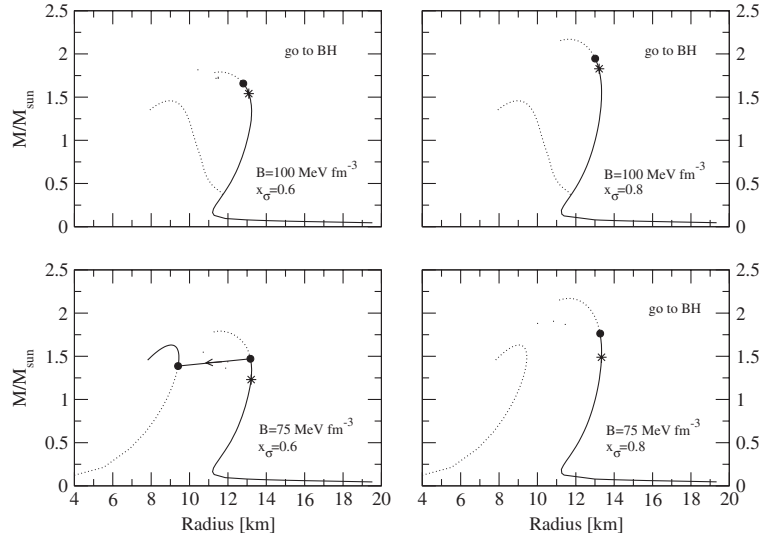


FIG. 4. Mass-radius relation for a pure HS described within the GM1 parametrization and that of the HYS or SS configurations for two values of the bag constant ($B = 75$ and 100 MeV/fm^3) and two values of the hyperon-meson coupling ($x_\sigma = 0.6$ and 0.8) and $m_s = 150 \text{ MeV}$ and $\alpha_s = 0$. The configuration marked with an asterisk represents in all cases the HS for which the central pressure is equal to P_0 . The conversion process of the HS, with a gravitational mass equal to M_{cr} , into a final HYS or SS is denoted by the full circles connected by an arrow. In all the panels σ is taken equal to 30 MeV/fm^2 .

M_{cr} configuration are quite separated, contrary to what was observed with QMC, Fig. 3.

The larger mass difference between the star with the central pressure P_0 and the one with the M_{cr} occurs when these stars have small masses. A small change in the central energy density corresponds to a large change in the mass. If instead of plotting the MR graph we would have plotted the corresponding mass-central pressure graph a larger difference between these two configurations

would be expected. This is seen in Figs. 5 and 6 where the mass-pressure curves for the family of stars obtained, respectively, within QMC and GM1 are plotted for two bag constants and two values of the surface tension ($\sigma = 10$ and 30 MeV/fm^2). We conclude that when the M_{cr} star is almost on top of the P_0 star in the MR curves, these stars lie on or close to the plateau that contains the maximum mass configuration. A large separation between these two configurations corresponds to a phase transition which

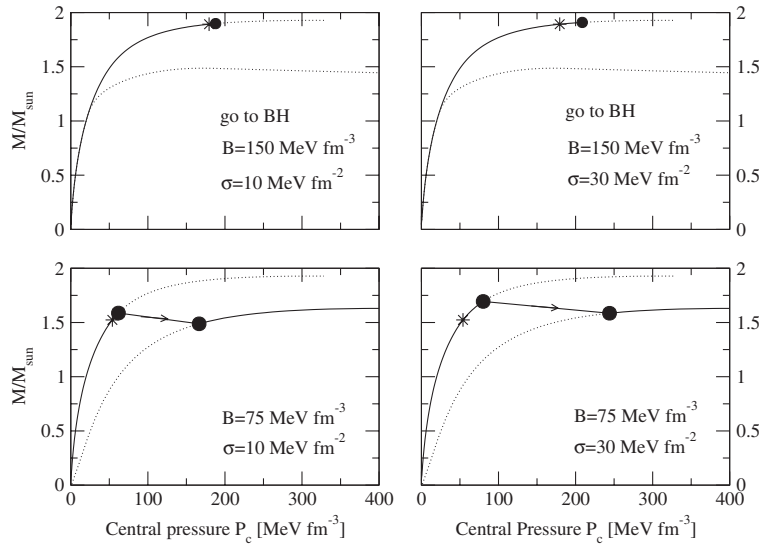


FIG. 5. Mass-pressure relation for a pure HS described within the QMC model and that of the HYS or SS configurations for two values of the bag constant (75 and 100 MeV/fm^3) and $m_s = 150 \text{ MeV}$ and $\alpha_s = 0$. The configuration marked with an asterisk represents in all cases the HS for which the central pressure is equal to P_0 . The conversion process of the HS, with a gravitational mass equal to M_{cr} , into a final HYS or SS is denoted by the full circles connected by an arrow. Two values of the surface energy σ were considered, 10 MeV/fm^2 (left) and 30 MeV/fm^2 (right).

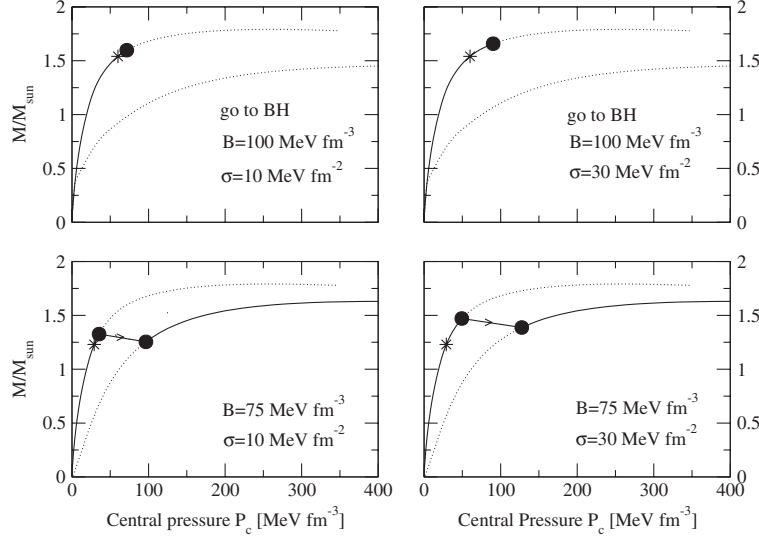


FIG. 6. The same as Fig. 5 for the GM1 parametrization with the $x_\sigma = 0.6$ hyperon coupling.

occurs during the rise of the MR curve before the plateau. Because of the softness of the QMC EOS, hyperons initiate at quite large energy densities and the star with the central P_0 pressure only occurs at high densities. We also conclude that a smaller surface tension hastens the transition and the critical mass is closer to the P_0 mass.

In Tables I, II, and III we give the gravitational (M_{cr}) and baryonic (M_{cr}^b) critical mass values for the hadronic star sequence, together with the central hyperon fraction ($f_{Y,\text{cr}} = n_Y/n_B$, i.e. the ratio between the total hyperon number density and the total baryon number density at the center of the critical mass star). We also report the value of the gravitational mass (M_{fin}) of the final quark star configuration and the total energy [18] $E_{\text{conv}} = (M_{\text{cr}} - M_{\text{fin}})c^2$ released in the stellar conversion process, assuming baryon mass conservation (i.e. no matter ejection) [18]. The gravitational ($M_{\text{QS,max}}$) and the baryonic ($M_{\text{QS,max}}^b$) mass of the maximum mass configuration for the quark (hybrid or strange) star sequence are also included. The value of the latter quantity is relevant to establish whether the critical mass hadronic star will evolve to a quark star ($M_{\text{cr}}^b < M_{\text{QS,max}}^b$) or will form a black hole ($M_{\text{cr}}^b > M_{\text{QS,max}}^b$). The entries in Tables I and II [31], and III are relative, respectively, to the GM1, GM3 and QMC equation of state for the hadronic phase. For the quark phase we consider four different values of bag constants, 75, 85, 100 and 150 MeV/fm³, and two different values for quark-hadron surface tension, 10 and 30 MeV/fm². Notice that for the quark matter parameter set adopted in the present work (see Sec. I), strange quark matter is absolutely stable [32,33] only for $B = 75$ MeV/fm³.

Some comments are in order: the critical masses increase with the increase of the hyperon couplings. This increase can be as large as $0.3\text{--}0.4M_\odot$ when x_σ changes from 0.6 to 0.8; the critical mass is also dependent on the particle content, namely, of the strangeness content, and

this explains the different relative positions for the different bag pressures of the QMC result which essentially corresponds to $x_\sigma = 0.7$. Because of the fact that the EOS for QMC is very soft, the hyperon onset occurs at quite high densities and therefore the critical mass is always quite high for this model. The critical mass increases with the bag constant because a larger bag constant corresponds to a stiffer quark EOS and therefore the phase transition to the quark phase will occur at larger densities. When the critical mass hadronic star is converted to a black hole, this is indicated in Tables I, II, and III with an entry BH, in the columns for M_{fin} and E_{conv} (no energy will be radiated as soon as the star passes the event horizon). Notice that, in the case of the GM3 model with $x_\sigma = 0.6$ and $B = 150$ MeV/fm³, there is no entry for the critical mass value (and for M_{cr}^b , M_{fin} , and E_{conv}) since in this case the nucleation time of the maximum mass hadronic star ($M_{\text{HS,max}}$) is much larger than 1 yr (i.e. the star is metastable with a *lifetime* comparable or much higher than the age of the Universe).

We observe from the results in Tables I and II, that increasing the value of the hyperon coupling constants (for fixed B and σ) reduces the central hyperon fraction ($f_{Y,\text{cr}}$) of the critical mass star, and increases the energy released during the conversion into a quark or hybrid star (for those configurations which will not form a black hole).

In Fig. 7, we show the internal composition for the hadronic star with a gravitational mass $M = 2.081M_\odot$ and radius $R = 12.6$ km, obtained using the GM1 parametrization with $x_\sigma = 0.8$. This star corresponds to the critical mass configuration when we consider $B = 150$ MeV/fm³ and $\sigma = 30$ MeV/fm² (see Table I). As we see, this star has a considerable central hyperon fraction ($f_{Y,\text{cr}} = 0.299$) and a wide hyperonic matter core which extends up to $R_Y \sim 8.7$ km. On the top of this core, one has a nuclear matter layer ($R_Y \leq r \leq R_{\text{crust}}$) with a

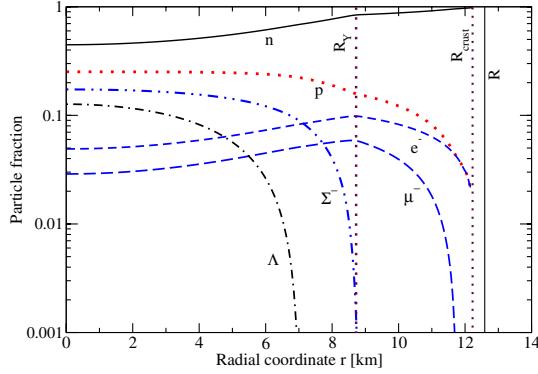


FIG. 7 (color online). The internal composition for an hadronic star with gravitational mass $M = 2.081M_{\odot}$ and radius $R = 12.6$ km, obtained with the GM1 equation of state with $x_{\sigma} = 0.8$. This star corresponds to the critical mass configuration when we consider $B = 150$ MeV/fm³ and $\sigma = 30$ MeV/fm² (see Table I). R_Y is the radius of the hyperonic matter stellar core. The nuclear matter layer extends between R_Y and R_{crust} . The crust extends between R_{crust} and R .

thickness of about 3.4 km. The stellar crust extends from R_{crust} up to R .

It has been argued by several authors [34–37] that if strange quark matter (SQM) is absolutely stable [32,33], then all compact stars are likely to be strange stars. The argument in favor of this thesis is the following: if the interstellar medium is sufficiently contaminated by *quark nuggets* (i.e. lumps of SQM), then the presence of a single quark nugget in the interior of a “normal” neutron star (hadronic star) is sufficient to trigger the conversion of the star to a strange star [33,34]. Likely the quark nugget contamination of the interstellar medium is the result of the merging of strange stars in binary systems [35,38]. Under these conditions, compact star progenitors could capture a quark nugget during their *lives* (i.e. during the various nuclear burning stages of the stellar evolution). Thus, according to this argument, a strange quark seed will be present in all newborn compact stars, and thus the conversion to a strange star will happen immediately, without a metastable hadronic star being formed first. This is a plausible scenario; however it would be relevant only for a few of the stellar models considered in our work, i.e. those relative to the value $B = 75$ MeV/fm³ for the bag constant (see Tables I, II, and III) for which SQM is absolutely stable, and will not have any effect upon the existence of metastable hadronic compact stars in all the other cases considered in the present work. The magnitude of the flux of quark nuggets in the interstellar medium (which is a crucial quantity for the validity of the scenario of Refs. [34–37]) has been estimated [35], making the assumption that all pulsars exhibiting glitches must be normal neutron stars (hadronic stars), not strange stars. This assumption is based primarily on the nearly total lack of models for the glitch phenomenon with strange stars (see anyhow Refs. [39,40]), while such models have

been quite successfully developed in the case of hadronic stars (see e.g. Refs. [41–44]). However, recent studies have established the possibility of an inhomogeneous crystalline color superconducting phase (Larkin-Ovchinnikov-Fulde-Ferrell phase) in the interior of strange stars (see [45,46] and references therein quoted), or the likely existence of a SQM crystalline crust in strange stars [47]. These late theoretical developments raise the possibility of explaining pulsar glitches with strange star based models, and thus require as useful a recalculation of the astrophysical limits of the flux of quark nuggets. The scenario discussed in the present work is an alternative to the scenario [34–37] according to which all compact stars are strange stars, which requires that SQM is absolutely stable.

V. CONCLUSIONS

It has been recently shown [11–15] that pure hadronic compact stars, above a threshold value of their gravitational mass, are metastable to the conversion to quark stars. In this work we have done a systematic study of the metastability of pure hadronic compact stars using different relativistic hadronic models for the equation of state of hadronic dense matter. In particular, we have used and compared the quark-meson coupling (QMC) model with those for the Glendenning-Moszkowski parametrization of the nonlinear Walecka model (NLWM). In the case of the QMC model, we have obtained that the region of metastability of pure hadronic stars is very narrow. For the GM model, we have investigated the effect of the hyperon couplings on the critical mass of the hadronic star sequence and on the stellar conversion energy. We have found that increasing the value of the hyperon coupling constants shifts the bulk transition point for quark deconfinement to higher densities, increasing the value of the critical mass for the hadronic stellar sequence, and thus makes the formation of quark stars less likely. The nucleonic EOS for QMC is very soft and therefore the onset of hyperons occurs at quite high densities, which gives rise to large critical masses. The conversion to a quark star will occur only for a small value of the bag constant. Finally we point out that both QMC and GM1 with the largest values of the hyperon-meson couplings predict *limiting masses* [12] which may be as high as 1.9 – $2.1M_{\odot}$.

These values would be able to describe highly massive compact stars, such as the one associated to the millisecond pulsars PSR B1516 + 02B [20], and nearly the one in PSR J1748-2021B [21].

ACKNOWLEDGMENTS

This work was partially supported by FEDER/FCT (Portugal) under Projects No. POCI/FP/63918/2005 and No. PTDC/FIS/64707/2006, by the Ministero dell’Università e della Ricerca (Italy), and by the European Science Foundation under Program No. 06-RNP-106.

- [1] J.E. Horvath, O.G. Benvenuto, and H. Vucetich, *Phys. Rev. D* **45**, 3865 (1992).
- [2] J.E. Horvath, *Phys. Rev. D* **49**, 5590 (1994).
- [3] M.L. Olesen and J. Madsen, *Phys. Rev. D* **49**, 2698 (1994).
- [4] M. Prakash, I. Bombaci, M. Prakash, P.J. Ellis, J.M. Lattimer, and R. Knorren, *Phys. Rep.* **280**, 1 (1997).
- [5] G. Lugones and O.G. Benvenuto, *Phys. Rev. D* **58**, 083001 (1998).
- [6] O.G. Benvenuto and G. Lugones, *Mon. Not. R. Astron. Soc.* **304**, L25 (1999).
- [7] I. Vidaña, I. Bombaci, and I. Parenti, *J. Phys. G* **31**, S1165 (2005).
- [8] F. Grassi, *Astrophys. J.* **492**, 263 (1998).
- [9] K. Iida and K. Sato, *Prog. Theor. Phys.* **98**, 277 (1997).
- [10] K. Iida and K. Sato, *Phys. Rev. C* **58**, 2538 (1998).
- [11] Z. Bereziani, I. Bombaci, A. Drago, F. Frontera, and A. Lavagno, *Astrophys. J.* **586**, 1250 (2003).
- [12] I. Bombaci, I. Parenti, and I. Vidaña, *Astrophys. J.* **614**, 314 (2004).
- [13] A. Drago, A. Lavagno, and G. Pagliara, *Phys. Rev. D* **69**, 057505 (2004).
- [14] G. Lugones and I. Bombaci, *Phys. Rev. D* **72**, 065021 (2005).
- [15] I. Bombaci, G. Lugones, and I. Vidaña, *Astron. Astrophys.* **462**, 1017 (2007).
- [16] A. V. Olinto, *Phys. Lett. B* **192**, 71 (1987).
- [17] H. Heiselberg, G. Baym, and C. J. Pethick, *Nucl. Phys. B, Proc. Suppl.* **24**, 144 (1991).
- [18] I. Bombaci and B. Datta, *Astrophys. J.* **530**, L69 (2000).
- [19] J.R. Oppenheimer and G.M. Volkoff, *Phys. Rev.* **55**, 374 (1939).
- [20] P.C.C. Freire, A. Wolszczan, M. van den Berg, and J.W.T. Hessels, *arXiv:0712.3826*.
- [21] P.C.C. Freire *et al.*, *arXiv:0711.0925*.
- [22] P.A.M. Guichon, *Phys. Lett. B* **200**, 235 (1988); K. Saito and A.W. Thomas, *Phys. Lett. B* **327**, 9 (1994).
- [23] P.A.M. Guichon, K. Saito, E. Rodionov, and A.W. Thomas, *Nucl. Phys.* **A601**, 349 (1996); K. Saito, K. Tsushima, and A.W. Thomas, *Nucl. Phys.* **A609**, 339 (1996); P.K. Panda, A. Mishra, J.M. Eisenberg, and W. Greiner, *Phys. Rev. C* **56**, 3134 (1997).
- [24] J.D. Walecka, *Ann. Phys. (N.Y.)* **83**, 491 (1974); B.D. Serot and J.D. Walecka, *Adv. Nucl. Phys.* **16**, 1 (1986).
- [25] N.K. Glendenning and S. Moszkowski, *Phys. Rev. Lett.* **67**, 2414 (1991).
- [26] E. Farhi and R.L. Jaffe, *Phys. Rev. D* **30**, 2379 (1984).
- [27] N.K. Glendenning, *Compact Stars* (Springer, New York, 2000).
- [28] D.P. Menezes and C. Providência, *Phys. Rev. C* **68**, 035804 (2003).
- [29] P.K. Panda, D.P. Menezes, and C. Providencia, *Phys. Rev. C* **69**, 025207 (2004).
- [30] H. Heiselberg, C. J. Pethick, and E.F. Staubo, *Phys. Rev. Lett.* **70**, 1355 (1993).
- [31] We have found a typo in one of the GM EOS coupling constants in the code used by the authors of Ref. [12]. In the present calculations, we have corrected this typo and we have increased the numerical accuracy of our code. This justifies the small differences between the present results and those reported in Ref. [12].
- [32] A.R. Bodmer, *Phys. Rev. D* **4**, 1601 (1971).
- [33] E. Witten, *Phys. Rev. D* **30**, 272 (1984).
- [34] C. Alcock, E. Farhi, and A. Olinto, *Astrophys. J.* **310**, 261 (1986).
- [35] J. Madsen, *Phys. Rev. Lett.* **61**, 2909 (1988).
- [36] O.G. Benvenuto and J.E. Horvath, *Mod. Phys. Lett. A* **4**, 1085 (1989).
- [37] R.R. Caldwell and J.L. Friedman, *Phys. Lett. B* **264**, 143 (1991).
- [38] J. Madsen, *arXiv:astro-ph/0612740*.
- [39] J.E. Horvath, *Int. J. Mod. Phys. D* **13**, 1327 (2004).
- [40] R.X. Xu, *Astrophys. J.* **596**, L59 (2003); R.X. Xu and A.Z. Zhou, *arXiv:astro-ph/0411018*.
- [41] P.W. Andeson and N. Itoh, *Nature (London)* **256**, 25 (1975).
- [42] R.I. Epstein and G. Baym, *Astrophys. J.* **328**, 680 (1988).
- [43] B. Link, R.I. Epstein, and G. Baym, *Astrophys. J.* **403**, 285 (1993).
- [44] P.B. Jones, *Phys. Rev. Lett.* **79**, 792 (1997); **81**, 4560 (1998).
- [45] M. Mannarelli, K. Rajagopal, and R. Sharma, *Phys. Rev. D* **76**, 074026 (2007).
- [46] R. Casalbuoni and G. Nardulli, *Rev. Mod. Phys.* **76**, 263 (2004).
- [47] P. Jaikumar, S. Reddy, and A.W. Steiner, *Phys. Rev. Lett.* **96**, 041101 (2006).